Turkish J. Eng. Env. Sci.
30 (2006) , 1 – 13.

A Computational Hydrodynamic and Heat Transfer Study in Turbulent Up-Flows of Dilute Slurries through a Concentric Annulus

Tülay A. OZBELGE[1], Ahmet N. ERASLAN[2]
[1] *Middle East Technical University, Department of Chemical Engineering*
Ankara-TURKEY
[2] *Middle East Technical University, Department of Engineering Sciences*
Ankara-TURKEY
e-mail: aeraslan@metu.edu.tr

Received 10.12.2004

Abstract

A computational model based on a continuum approach is developed to estimate the hydrodynamic and heat transfer characteristics of turbulent slurry up-flows through a concentric annulus. The dilute slurry is treated as a single phase fluid of variable physical and thermal properties in the flow area. Prandtl's mixing length model is used to obtain the closure equations of turbulence. Experimental solid density distribution data are incorporated in the model to estimate the local physical and thermal properties of the slurry in the radial direction. It is also shown that in the limiting case of zero solids loading, the present model fits well to the single phase heat transfer correlation and the flow data available in the literature.

Key words: Liquid-solid turbulent flow, Slurry heat transfer, Solids density profile, Solids loading.

Introduction

Multiphase flows are encountered in many industrial and engineering applications. In spite of the recent developments in experimental and computational techniques for 2-phase flows (Roco, 1996), it is still difficult to give reliable predictions of flow and heat transfer characteristics in these systems, because the problem is heavily dependent on the system geometry and the experimental parameters such as flow and particle Reynolds numbers, particle size, solids loading and radial solid density distribution (RSDD). Most of the existing correlations are entirely empirical, yielding poor accuracies when applied to systems other than those for which they are obtained (Julian and Duckler, 1965; Rose and Duckworth, 1996).

Hydraulic transport has been used since the 1920s for the transportation of solid materials (Michaelides, 1986) due to its low operational and maintenance costs. Solid particles may have different radial concentration profiles depending on the properties of the solids and the conveying liquid at different operating conditions in various geometries (Sadatomi et al., 1982; Alajbegovic et al., 1994). Particle-wall, particle-particle, and particle-eddy interactions are important factors that affect the concentration or density profiles of solids at a cross section of the conduit perpendicular to the flow direction. It has been reported that the radial location of maximum slurry density in laminar up-flows through a concentric annulus has an importance in determining the flow and heat transfer characteristics of dilute slurries (Eraslan and Ozbelge, 2003).

Particulate flows have further importance in heat transfer fields. Energy and material saving considerations have led to advanced design studies to manufacture more efficient heat transfer equipment. Heat transfer can be enhanced by the addition of micron-size solid particles into gases or liquids at small vol-

umetric fractions due to the thinning of the viscous sublayer by solids and occurrence of high thermal conductivity in that layer (Boothroyd, 1971). Various heat transfer enhancement techniques will probably be sought with increasing frequency and importance owing to the increasing shortages of energy and material in the near future; in parallel to this, it is expected that the demand for accurate theoretical predictions will increase as well. As a matter of fact, numerous experimental and theoretical studies in horizontal and vertical pipe geometries have already been carried out (Brandon and Thomas, 1970; Plass and Molerus, 1974; Ozbelge and Somer, 1988; Park et al., 1989; Ozbelge, 1993; Hestroni and Rozenblit, 1994) since turbulence in particulate flows is also an important factor for enhancing the convective heat transfer. The objective here is to perform a modeling study with sufficient accuracy and low computational cost to estimate the flow and heat transfer characteristics of dilute liquid-solid up-flows in a concentric annulus. It is thought that it is worth the effort, to enrich the literature with a theoretical study of turbulent slurry heat transfer in the annulus geometry. For the verification of the predictions, the experimental heat transfer data available in the literature (Ozbelge and Köker, 1996) are used.

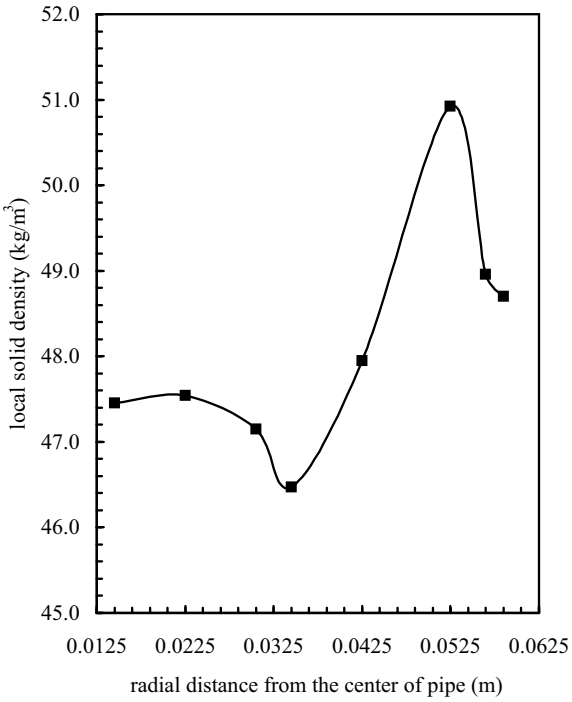

Figure 1. Experimental radial solid density distribution for $d_p = 0.165$ mm, $C_f = 0.6\%$ (V/V), aspect ratio = 0.2, $D_H = 0.1$ m and $Re = 8970$.

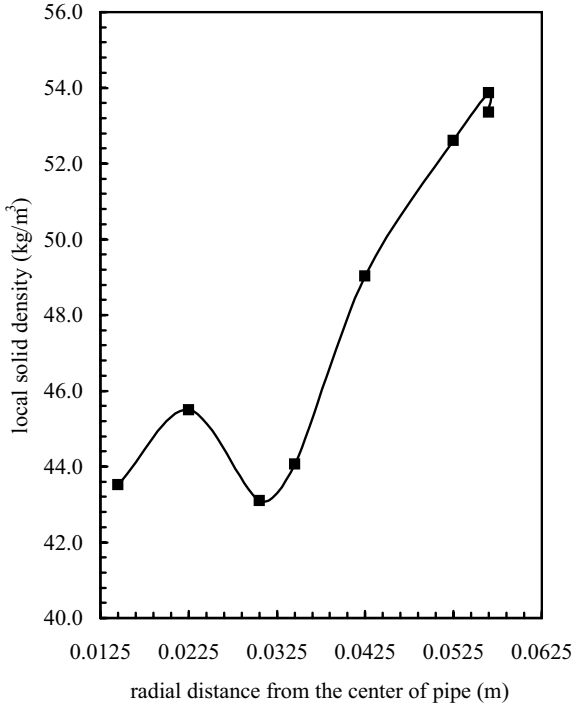

Figure 2. Experimental radial solid density distribution for $d_p = 0.138$ mm, $C_f = 0.8\%$ (V/V), aspect ratio = 0.2, $D_H = 0.1$ m and $Re = 15,200$.

Computational Model

Representative RSDD data from previous work (Ozbelge and Beyaz, 2001) are given in Figures 1-3, where the experimental local solid densities are shown by the symbols and the least-square fits to the data are given by solid lines for different particle diameters of 0.165, 0.138 and 0.230 mm, slurry Reynolds numbers of 8970, 15,200 and 16,400 and the feed solid concentrations of $C_f = 0.6$, 0.8% and 1.8 % (V/V), respectively, because for the solution of the present problem RSDD data or functions are needed. The density, heat capacity and thermal conductivity of the feldspar ($K_2O \cdot Al_2O_3 \cdot SiO_2$) particles used in the experiments are $\rho_p = 2500$ kg/m^3, $c_p = 836.8$ J/kg-K, and $k_p = 1.09$ W/m-K, respectively.

In Figure 4, the schematics of a vertical concentric annulus is shown with a typical turbulent single phase velocity profile. System coordinates can be defined as z and r, with z being the flow direction.

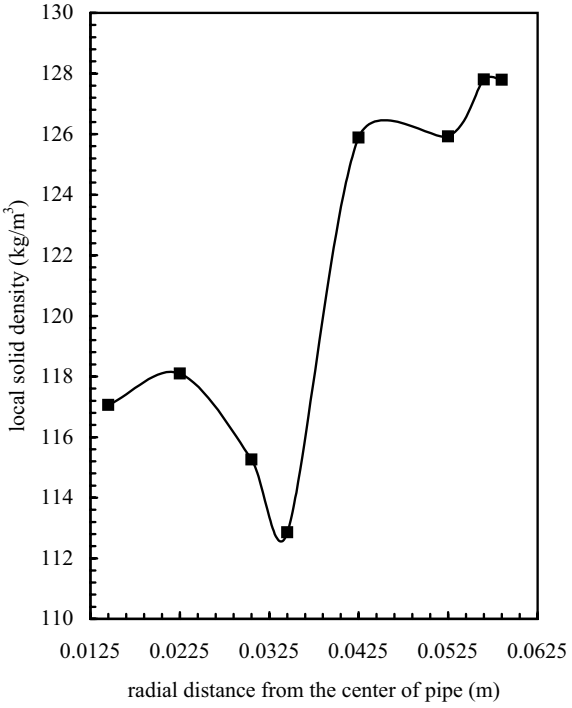

Figure 3. Experimental radial solid density distribution for $d_p = 0.230$ mm, $C_f = 1.8\%$ (V/V), aspect ratio $= 0.2$, $D_H = 0.1$ m and $Re = 16,400$.

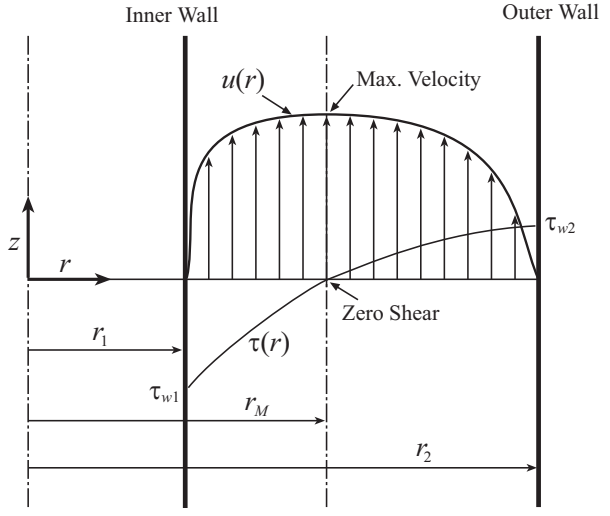

Figure 4. The geometry of the annulus; typical velocity and shear stress profiles in turbulent single phase flow.

The model developed in this work is based on the following assumptions: (i) one-dimensional incompressible steady flow with a fully developed velocity profile, (ii) no wall-roughness exists, (iii) dilute slurry, having less than 10% (V/V) solid particles with uniform sizes in the range of 64-230 μm, behaves as a Newtonian fluid as justified by Zandi (1971) for dilute liquid-solid suspension flows; moreover, the slip between the phases will be negligible (Mehta et al., 1957) (iv) slurry is treated as a single phase fluid with locally variable physical and thermal properties according to the radial distribution of solid particles in the liquid phase, (v) pressure gradient is defined as positive in the flow direction, (vi) the forced convective heat transfer problem is solved for the boundary conditions of constant temperature at the inner wall and zero heat flux at the outer wall (insulated wall).

Hydrodynamics

A momentum balance over a shell of slurry flowing upward through the annulus results in

$$-\frac{1}{r}\frac{d}{dr}(r\,\tau) = -\frac{dP}{dz} + \rho_m g \tag{1}$$

where $\rho_m(r)$ is the density distribution function of the variable density single-phase fluid (VDSPF), which is obtained using the RSDD, $\rho_s(r)$, and the following volumetric relation between the phases (Ozbelge and Beyaz, 2001),

$$\begin{aligned} \rho_m(r) &= \rho_l\,[1 - \phi_s(r)] + \rho_p\,\phi_s(r) \\ &= \rho_l\,[1 - \phi_s(r)] + \rho_s(r) \end{aligned} \tag{2}$$

where ρ_l, ρ_p, $\phi_s(r)$ and $\rho_s(r)$ are the density of the liquid, density of the particle, local volume fraction of solids and local solid density in the mixture, respectively. In Eq. (2), $\phi_s = 0$ corresponds to the case of zero solids loading. Integrating Eq. (1) from r_1 to r and rearranging yields the shear stress distribution in annular flow,

$$\tau(r) = \frac{\tau_{w1} r_1}{r} + \frac{1}{2}\frac{dP}{dz}\left(\frac{r^2 - r_1^2}{r}\right) - \frac{g}{r}\int_{r_1}^{r} \rho_m r\,dr \tag{3}$$

Here, the total shear stress, τ, consists of laminar and turbulent shear stress components as

$$\tau(r) = \tau^L(r) + \tau^T(r) \tag{4}$$

where $\tau^L(r)$, being negligibly small, can be neglected when compared with the turbulent shear stress component $\tau^T(r)$; thus for turbulent flow, Eq. (4) becomes, $\tau(r) \approx \tau^T(r)$. Based on the previous studies (Hinze, 1959; Schlichting, 1968; Michaelides and

Farmer, 1984; Michaelides, 1986), the mean turbulent shear stress can be written for the VDSPF as

$$\tau^T = -\overline{(u+u')(v+v')(\rho_m+\rho'_m)} \tag{5}$$

where the primed terms stand for variables having fluctuations in time and the terms with a bar stand for the time-averaged variables. For a fully developed one-dimensional flow $v = 0$, hence Eq. (5) reduces to the following form

$$\tau^T = -(\rho_m\overline{u'v'} + u\overline{\rho'_m v'} + \overline{\rho'_m u'v'}) \tag{6}$$

The third term on the right hand side of Eq. (6) represents the third-order fluctuations, which can be neglected when compared to the other terms (Hinze, 1959; Schlichting, 1968; Michaelides and Farmer, 1984; Michaelides, 1986). Closure equations are needed to express the time-averaged primed terms, that is, the Reynolds stresses. Using the Prandtl's mixing length hypothesis (Hinze, 1959; Schlichting, 1968), closure equations take the following forms:

$$\overline{u'v'} = -l_u l_v \left|\frac{du}{dr}\right| \frac{dv}{dr} \tag{7}$$

$$\overline{\rho'_m v'} = -l_\rho l_v \left|\frac{d\rho_m}{dr}\right| \frac{dv}{dr} \tag{8}$$

where l_u, l_v and l_ρ are the mixing lengths for velocity and density, respectively. Due to the lack of experimental data on different mixing lengths, all the mixing lengths are assumed approximately equal to each other as these approximations have been used successfully by numerous previous researchers (Michaelides and Farmer, 1984; Michaelides, 1986); therefore, we may write

$$\overline{u'v'} = -l^2 \left|\frac{du}{dr}\right| \frac{du}{dr} \tag{9}$$

$$\overline{\rho'_m v'} = -l^2 \left|\frac{d\rho_m}{dr}\right| \frac{du}{dr} \tag{10}$$

Hence, the turbulent shear stress becomes

$$\tau(r)^T = l^2 \left[\rho_m \left|\frac{du}{dr}\right| + u\left|\frac{d\rho_m}{dr}\right|\right] \frac{du}{dr} \tag{11}$$

For the estimation of mixing length l, the Prandtl mixing length assumption (Hinze, 1959; Schlichting, 1968), given by $l = \kappa y$, is used, with κ being the von Karman constant, and y the vertical distance from each wall. In the turbulent flow of dilute slurries through an annulus, the flow area can be divided into 2 regions, inner and outer, and the vertical distance y from each wall is defined accordingly. After experimenting with different definitions of y in both regions, the following are used in this work, giving the best predictions,

$$y = r - r_1 \quad \text{for} \quad r_1 \le r \le r_M \tag{12}$$

$$y = r_2 - r \quad \text{for} \quad r_M \le r \le r_2 \tag{13}$$

where r_M stands for the radial location of maximum velocity and zero shear. Furthermore, in the inner wall region ($r_1 \le r \le r_M$) of the annulus $du/dr > 0$ and hence $|du/dr| = +du/dr$, and, by similar reasoning, in the outer wall region ($r_M \le r \le r_2$), $|du/dr| = -du/dr$. Accordingly, the governing equations for the inner and outer wall regions take the following forms:

$$\left[\kappa^2(r-r_1)^2\rho_m\right]\left(\frac{du}{dr}\right)^2 + \left\{\kappa^2(r-r_1)^2\left|\frac{d\rho_m}{dr}\right|\right\} u\frac{du}{dr} - \frac{\tau_{w1}r_1}{r} - \frac{1}{2}\frac{dP}{dz}\left(\frac{r^2-r_1^2}{r}\right) + \frac{g}{r}\int_{r_1}^{r}\rho_m r dr = 0 \tag{14}$$

$$-\left[\kappa^2(r_2-r)^2\rho_m\right]\left(\frac{du}{dr}\right)^2 + \left\{\kappa^2(r_2-r)^2\left|\frac{d\rho_m}{dr}\right|\right\} u\frac{du}{dr} - \frac{\tau_{w1}r_1}{r} - \frac{1}{2}\frac{dP}{dz}\left(\frac{r^2-r_1^2}{r}\right) + \frac{g}{r}\int_{r_1}^{r}\rho_m r dr = 0 \tag{15}$$

Julian and Dukler (1965) have reported that the von Karman constant does not deviate significantly from 0.4 with solids loading for dilute gas-solid flows. However, Michaelides and Farmer (1984) proposed a correlation for the von Karman constant as a function of solids concentration and liquid-solid mixture velocity. In the present study, this constant varied within the range of 0.38-0.42 depending on the variables in their correlation and that also helped the exact matching of the inner and outer wall region velocity profiles at the radial location of maximum velocity and/or zero shear stress. The above-given equations for the inner and outer wall regions of the annulus can be cast into the general form

$$\alpha\left(\frac{du}{dr}\right)^2 + \beta u\frac{du}{dr} + \gamma = 0 \tag{16}$$

Using forward differences for the inner wall region

$$\left(\frac{du}{dr}\right)_i = \frac{u_{i+1} - u_i}{\Delta r} \tag{17}$$

and backward differences for the outer wall region,

$$\left(\frac{du}{dr}\right)_i = \frac{u_i - u_{i-1}}{\Delta r} \tag{18}$$

Equations (14) and (15) are then discretized. For N grid points in the radial direction, making use of the boundary conditions $u_1 = u(r_1) = 0$ and $u_N = u(r_2) = 0$, a system of $N-2$ nonlinear equations is obtained. In addition to $N-2$ unknown velocities at the grid nodes, these equations contain 2 more unknowns, namely r_M and dP/dz. Two more equations can be written for the determination of totally N unknowns. These additional equations are

$$u^I(r_M) = u^O(r_M) \quad \text{and} \quad \left(\frac{du}{dr}\right)^I_{r=r_M} = \left(\frac{du}{dr}\right)^O_{r=r_M} \tag{19}$$

where the superscripts I and O denote the inner and outer wall regions, respectively. Starting with an assigned value of inner wall shear stress τ_{w1} and reasonable initial estimates for the unknowns from the authors' previous work (Eraslan and Ozbelge, 2003), the resulting system of N nonlinear equations is solved iteratively using the Powell hybrid method (Garbow et al., 1964). During the iterations, the number of grids in both regions ($r_1 < r \leq r_m$ and $r_m \leq r < r_2$) are adjusted so that the element sizes in both are equal. Once the fully developed turbulent velocity profile in the annulus is determined, various flow-related parameters are calculated. These parameters are defined as follows:

frictional pressure gradient:

$$\left(\frac{dP}{dz}\right)_{f_m} = \frac{dP}{dz} - \langle \rho_m \rangle g \tag{20}$$

friction factor:

$$f_m = \frac{D_H \left(dP/dz\right)_{f_m}}{2 \langle u \rangle^2 \rho_m} \tag{21}$$

slurry Reynolds number:

$$\mathrm{Re} = \frac{\langle u \rangle \langle \rho_m \rangle D_H}{\langle \mu_m \rangle} \tag{22}$$

in which $D_H = 2(r_2 - r_1)$ is the hydraulic diameter, and $\langle \mu_m \rangle$ the average slurry viscosity given by (Kofanov, 1964)

$$\langle \mu_m \rangle = \mu_l \left[1 + 2.5 \times \left(\frac{\langle \rho_m \rangle - \rho_l}{\rho_p - \rho_l}\right)\right] \tag{23}$$

and the other averages over the cross section are obtained from

$$\langle \phi \rangle = \frac{2 \int_{r_1}^{r_2} \phi(r) r dr}{r_2^2 - r_1^2} \tag{24}$$

Heat transfer

The energy equation for fully developed turbulent flow through an annulus can be expressed as (Bird et al., 2002)

$$\rho_m c_m u \frac{\partial T}{\partial z} = -\frac{1}{r}\frac{\partial}{\partial r}\left[r\left(q^L + q^T\right)\right] \tag{25}$$

in which c_m is the slurry heat capacity, and q^L and q^T are the laminar and turbulent heat fluxes, respectively. The slurry heat capacity c_m is approximated by (Michaelides, 1986)

$$c_m(r) = c_l\left[1 - X_s(r)\right] + c_p X_s(r) \tag{26}$$

where c_l and c_p are the specific heat values of liquid and solid particles, respectively. $X_s(r)$ is the local mass fraction of solids in the liquid phase, which can be expressed in terms of the local volume fraction of solids in the liquid phase:

$$X_s(r) = \frac{\rho_p}{\rho_m(r)}\phi_s(r) \tag{27}$$

The laminar heat flux is given by

$$q^L = -k_m \frac{\partial T}{\partial r} \tag{28}$$

where the thermal conductivity of the liquid-solid mixture k_m can be approximated by Smith and Paradi (1982) as

$$k_m(r) = k_l\left[\frac{2k_l + k_p - 2\phi_s(r)\left(k_l - k_p\right)}{2k_l + k_p + \phi_s(r)\left(k_l - k_p\right)}\right] \tag{29}$$

In this equation, k_l and k_p are the thermal conductivities of liquid and solid particles. Using an approach similar to that in the hydrodynamics section, the turbulent heat flux can be written for the VD-SPF as (Michaelides, 1986)

$$q^T = -(\rho_m c_m \overline{T'v'} + T\rho_m \overline{c_m' v'} + T c_m \overline{\rho_m' v'}) \tag{30}$$

According to Prandtl's mixing length hypothesis (Hinze, 1959; Schlichting, 1968), the closure equations are

$$\overline{T'v'} = -l_T l_v \left|\frac{dT}{dy}\right| \frac{dv}{dy} \tag{31}$$

$$\overline{c'_m v'} = -l_c l_v \left|\frac{dc_m}{dy}\right| \frac{dv}{dy} \tag{32}$$

where l_T and l_c are the mixing lengths for temperature and heat capacity, respectively. Assuming equal mixing length scales we write

$$\overline{T'v'} = -l^2 \left|\frac{dT}{dy}\right| \frac{du}{dy} \tag{33}$$

$$\overline{c'_m v'} = -l^2 \left|\frac{dc_m}{dy}\right| \frac{du}{dy} \tag{34}$$

finally, the turbulent heat flux takes the form

$$q^T = l^2 \left[\rho_m c_m \left|\frac{dT}{dr}\right| + T\rho_m \left|\frac{dc_m}{dr}\right| + Tc_m \left|\frac{d\rho_m}{dr}\right|\right] \frac{du}{dr} \tag{35}$$

with

$$l^2 = \kappa^2 (r - r_1)^2 \quad \text{for} \quad r_1 \le r \le r_M \tag{36}$$

$$l^2 = \kappa^2 (r_2 - r)^2 \quad \text{for} \quad r_M \le r \le r_2 \tag{37}$$

The energy equation (25) can be put into the general form after substitution of laminar and turbulent heat fluxes as

$$\rho_m c_m u \frac{\partial T}{\partial z} = \alpha \frac{\partial^2 T}{\partial r^2} + \beta \frac{\partial T}{\partial r} + \gamma T \tag{38}$$

This equation is solved numerically, subject to the inlet and boundary conditions

$$T(r,0) = T_{in} \; T(r_1, z) = T_{w1} \text{ and } \left.\frac{\partial T(r,z)}{\partial r}\right|_{r=r_2} = 0$$

The discretization of Eq. (38) is achieved using the following backward and central differences for the derivatives:

$$\left(\frac{\partial T}{\partial z}\right)_j = \frac{T_j - T_j^*}{\Delta z} \tag{39}$$

$$\begin{aligned} \left(\frac{\partial T}{\partial r}\right)_i &= \frac{T_{i+1} - T_{i-1}}{2\Delta r} \text{ and} \\ \left(\frac{\partial^2 T}{\partial r^2}\right)_i &= \frac{T_{i+1} - 2T_i + T_{i-1}}{\Delta r^2} \end{aligned} \tag{40}$$

in which T_i^* denotes the temperature at $r = r_i$ and $z_j = z_j - \Delta z$. At any axial location Eq. (38) reduces to the linear algebraic system

$$C_i T_{i-1} + A_i T_i + B_i T_{i+1} = D_i \tag{41}$$

Gaussian elimination solution of this system is carried out by using the well-known tri-diagonal matrix algorithm.

Local heat transfer coefficient $h(z)$ and the Nusselt number $Nu(z)$ in the flow direction are calculated from

$$h(z) = \frac{k_m \frac{\partial T}{\partial r}\big|_{r=r_1}}{(T_b - T_{w1})} \tag{42}$$

$$Nu(z) = \frac{h(z)\; D_H}{k_m(r_1)} \tag{43}$$

where T_b is the local bulk fluid temperature, which is calculated using

$$T_b(z) = \frac{\int_{r_1}^{r_2} T(r,z)\, u(r)\, r dr}{\int_{r_1}^{r_2} u(r)\, r dr} \tag{44}$$

Results and Discussion

The predictions are obtained for dilute water-feldspar slurries in turbulent up-flows through an annulus with an aspect ratio of 0.2, hydraulic diameter of 0.1 m, and test section length of 1.22 m for which the RSDDs are available (Ozbelge and Beyaz, 2001), because for the solution of the present problem, RSDD data or functions are needed. The experimental results reported by Ozbelge and Beyaz (2001) are used for this purpose. In these experiments, an invasive technique of inserting a specially designed concentration probe (Ozbelge and Somer, 1988) into the flow area, in the fully developed flow region, is applied to measure the radial local solid densities. As given in the literature (McCabe et al., 1995), an entrance length of 45-50 times the hydraulic diameter of the annulus is allowed up to the test section in the set-up to ensure a fully developed flow. Although the non-invasive or non-intrusive measurements of local solid densities are more reliable, these are not available for liquid-solid flows in an annulus; moreover, the use of this probe has

yielded consistent trends in RSDDs, where the local solid densities increase from the inner wall to the outer wall of the annulus. They could not be measured within approximately 2 mm distances from the walls due to the wall thickness of the probe. As a result, the existence of a particle-free zone in the close vicinity of each wall is not clearly known. In addition, past experimental studies on single-phase turbulent flows (Brighton and Jones, 1964; Bird et al., 2002) and heat transfer (Ozbelge and Köker, 1996) in concentric annuli were used as check points to which the 2-phase flow results would reduce at zero solids loading.

Hydrodynamics

Two sets of experimental velocity data for single-phase flows have been taken from Brighton and Jones (1964); the first one is for a flow Reynolds number of 65,000 in an annulus with an aspect ratio of 0.375, and the other is for a Reynolds number of 89,000 and aspect ratio of 0.125. The dimensionless velocity profile predicted in this work for a Reynolds number of 75,480 and an aspect ratio of 0.2 was compared with these data (Brighton and Jones, 1964) in Figure 5, where the predicted dimensionless velocity profile is found to be located between the 2 experimental profiles, indicating a satisfactory agreement between the present hydrodynamic predictions and those in the literature.

For the VDSPF, plots of velocity and shear stress profiles obtained at a Reynolds numbers of 10,000 and inlet slurry temperature of 25 °C for various values of average solids loading, $\overline{\phi}_s$, are shown in Figures 6 and 7, respectively. In performing these calculations, zero solid density is assumed at each wall (Michaelides, 1986). As seen in these figures, the predicted turbulent velocity profile is flatter than that of laminar slurry flow in the same geometry (Eraslan and Ozbelge, 2003) and no reverse flow occurs even in the regions of the annular area where the local solid densities are relatively higher as observed in the RSDDs (Figures 1-3). This is due to the fact that the solids conveying capacity of the liquid phase is naturally higher in turbulent flow than that in laminar slurry flow. In Figure 6, it can be observed that the maximum velocity increases as the average solids loading (ASL) increases and the radial location of maximum velocity (or zero shear) approaches the inner wall of the annulus. As seen in Figure 7, the absolute values of inner and outer wall shear stresses are greater than the corresponding values in laminar slurry flows (Eraslan and Ozbelge, 2003), which is an expected result, as the wall shear stresses are directly related to the Reynolds number. Furthermore, these values increase with decreasing ASL at the same Reynolds number.

In Figure 8, the dimensionless radial location of maximum velocity (or zero shear), r^*_M, is plotted with respect to ASL, with the Reynolds number being a parameter. At constant Reynolds number, when the ASL is increased, the r^*_M value decreases, i.e. the radial location of maximum velocity approaches the inner wall. For a constant density single-phase fluid (CDSPF), r^*_M remains constant at 0.42075 regardless of the Reynolds number, which is slightly lower than that of laminar slurry flow (Eraslan and Ozbelge, 2003). However, for the VDSPF, r^*_M increases with increasing Reynolds number at the same ASL, and decreases with increasing ASL at a constant Reynolds number.

Figure 9 shows the dimensionless slurry frictional pressure gradient versus Reynolds number at different ASLs, where the pressure gradient increases with increasing ASL at the same Reynolds number. However, keeping the solids content constant, the normalized frictional 2-phase pressure gradient decreases with increasing Reynolds number. Figure 10 gives the dimensionless slurry friction factor versus Re plot, with ASL being a parameter. The trend of each curve at each constant ASL agrees with the well-known Moody diagram of CDSPF (Bird et al., 2002).

The effect of inlet temperature on physical properties is investigated as these properties directly affect the hydrodynamics of the system. In Figures 11 and 12, the dimensionless velocity profiles are plotted at a Reynolds number of 20,000 in both figures, but the inlet slurry temperature being 25 °C and 50 °C, respectively. In Figure 11, the dimensionless maximum velocity at ASL = 15 (% V/V) is around 1.38, while this value increases to almost 1.5 in Figure 12 for the same ASL at an inlet temperature of 50 °C. Furthermore, in the latter figure, a reverse flow is observed in the outer wall region of the annulus at an ASL of 15% (V/V); however, the reverse flow does not occur at the same ASL for a lower inlet temperature of 25 °C. That is, as the inlet temperature is increased, the solids conveying capacity of the liquid phase decreases. This can be attributed to the increasing terminal fall velocity of solid particles with the decreasing viscosity of the liquid as the temperature increases.

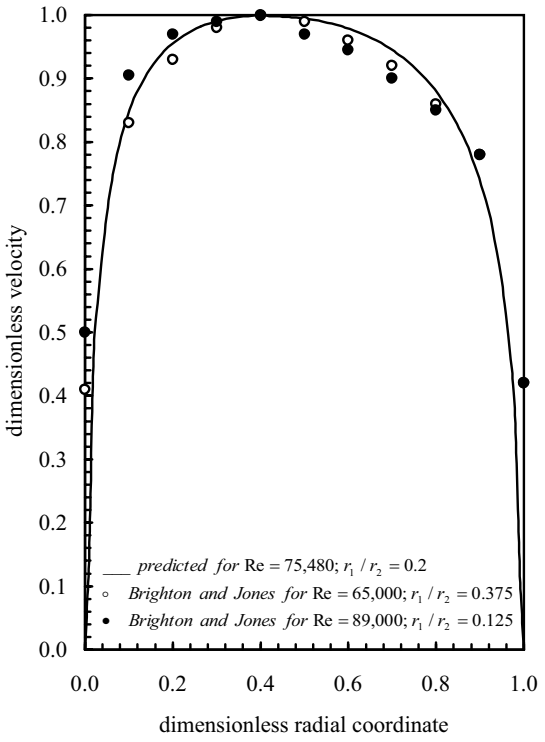

Figure 5. Comparison of predicted velocity profile with those in the literature for single phase turbulent flow (Smith and Paradi, 1982).

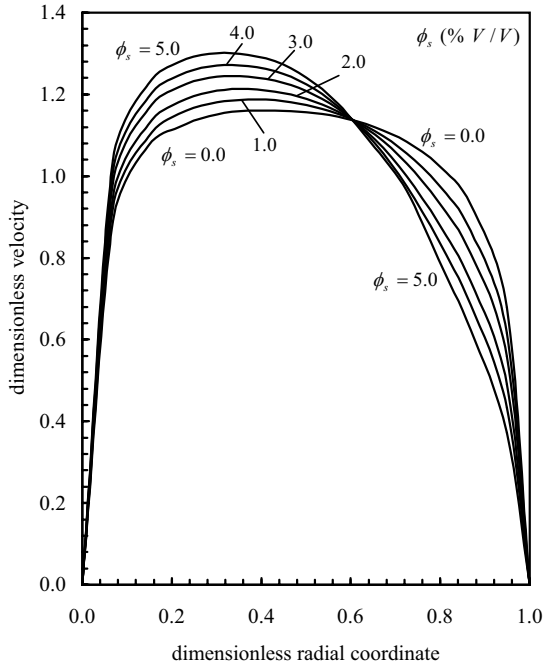

Figure 6. Slurry velocity profile at $Re = 10,000$ and $T_{in} = 25$ °C for different values of ASL ($\overline{\phi}_s$).

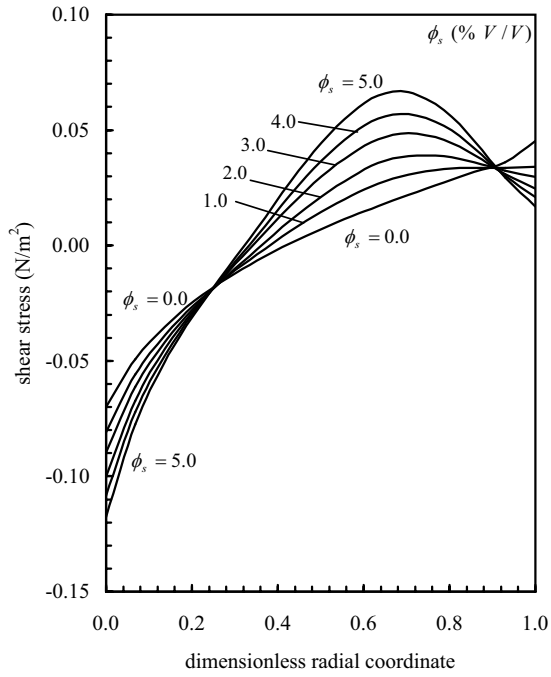

Figure 7. Slurry shear stress profile at $Re = 10,000$ and $T_{in} = 25$ °C for different values of ASL ($\overline{\phi}_s$).

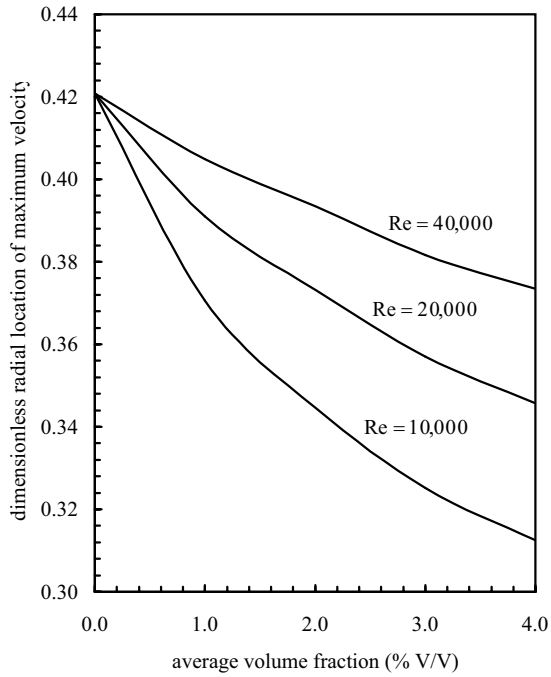

Figure 8. Dimensionless radial location of maximum velocity vs. ASL, for different values of Reynolds number.

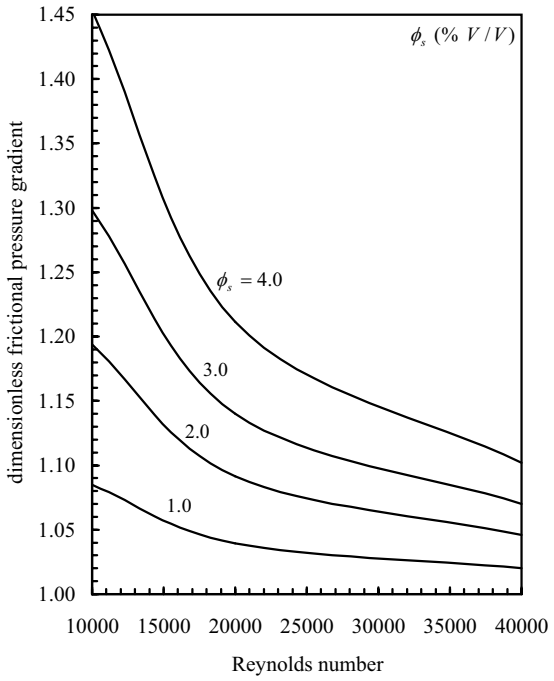

Figure 9. Dimensionless slurry pressure gradient due to friction vs. Reynolds number for different values of ASL ($\overline{\phi}_s$).

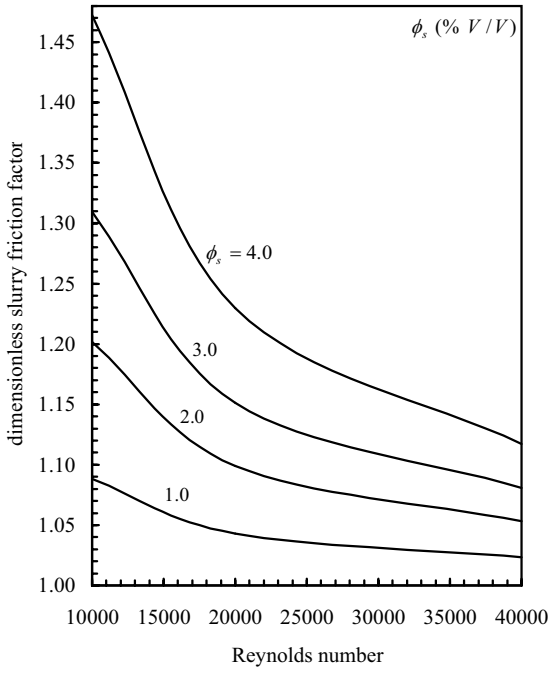

Figure 10. Dimensionless slurry friction factor vs. Reynolds number for different values of ASL ($\overline{\phi}_s$).

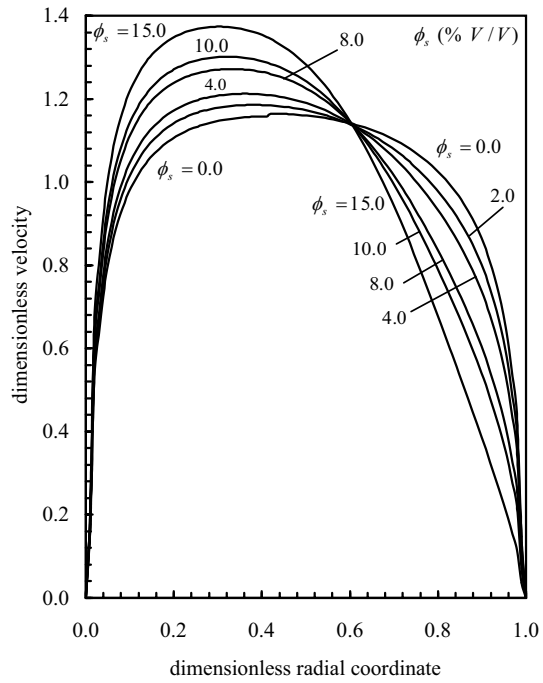

Figure 11. Dimensionless slurry velocity profile at $Re = 20,000$ and $T_{in} = 25$ °C for different values of ASL ($\overline{\phi}_s$).

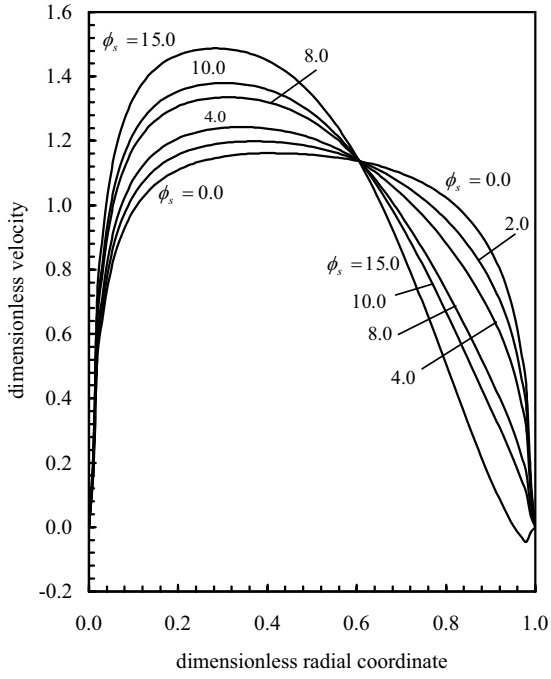

Figure 12. Dimensionless slurry velocity profile at $Re = 20,000$ and $T_{in} = 50$ °C for different values of ASL ($\overline{\phi}_s$).

Heat transfer

In Figure 13, heat transfer enhancement as a ratio of average slurry Nusselt number to that of single water phase in the test section of 1.22 m, (Nu_m/Nu_w), versus dimensionless axial distance (z/L) is plotted at various ASLs for the slurry inlet temperature of 50 °C and constant inner wall temperature of 10 °C. The calculations were performed for a test section length of 1.22 m in order to compare the predicted results with the previous experimental study in the same system (Ozbelge and Köker, 1996; Ozbelge, 2001). In turbulent flow, the slurry Nusselt numbers are greater than those of water flow at the same operating conditions, and the Nu_m/Nu_w values increase with increasing ASL at each axial distance, keeping the Reynolds number constant. This indicates that the introduction of solid particles into the system enhances the heat transfer (Ozbelge, 2001). Although Nu_m values in the turbulent slurry flows are much higher than those of laminar slurry flows predicted in our previous work (Eraslan and Ozbelge, 2003), the calculated heat transfer enhancement ratios (Nu_m/Nu_w) in this study are slightly lower than those of laminar slurry flows. This leads to the conclusion that the heat transfer enhancement or the effect of solids on the heat transfer characteristics of slurries is more significant in laminar flow or at lower Reynolds numbers. This is due to the fact that the stagnant area (similar to that of the viscous boundary layer in turbulent flow) is thicker in laminar flow and that particles spend more time in the wall regions and therefore the effect of the addition of particles on hydrodynamics and heat transfer is more significant in laminar slurry up-flows in an annulus. The effect of solids on the heat transfer mechanism in turbulent water-feldspar up-flows through annuli with different aspect ratios and for various particle sizes has been discussed in detail elsewhere (Ozbelge, 2001).

To investigate the effect of operating conditions on the heat transfer results, the higher inlet slurry temperature of 70 °C is studied, and the predicted Nu_m/Nu_w values with respect to z/L are plotted in Figure 14 for various ASLs. In comparing Figure 13 with Figure 14, it can be seen that the heat transfer enhancement ratios are higher at a higher inlet slurry temperature at the same ASL. Hence, increasing the inlet temperature favors heat transfer enhancement. One other important point was that it was not possible to calculate the slurry Nusselt number for an ASL of 11%(V/V) and 12.5%(V/V) for an inlet temperature of 70 °C (Figure 14), although it was possible for an inlet slurry temperature of 50 °C (Figure 13), keeping the other operating conditions constant. This is due to the reverse flow effect caused by increasing the inlet slurry temperature as discussed in the hydrodynamic section of this study.

In Figure 15, the plot of heat transfer enhancement ratio versus ASL at different Reynolds numbers is shown. An increase in ASL has a positive effect on the heat transfer enhancement ratio at a constant Reynolds number. On the other hand, heat transfer enhancement becomes less significant as the Reynolds number is increased from 10,000 to 40,000. It was reported that (Ozbelge, 2001), at high slurry Reynolds numbers such as around 45,000, a decrease in enhancement ratio was attributed to the high momentum gain by the particles in the direction of flow that prevented their lateral motion, thus decreasing the thinning effect on the viscous boundary layer; it was added that this effect could be compensated for by the increasing number density of the solid particles at high ASLs.

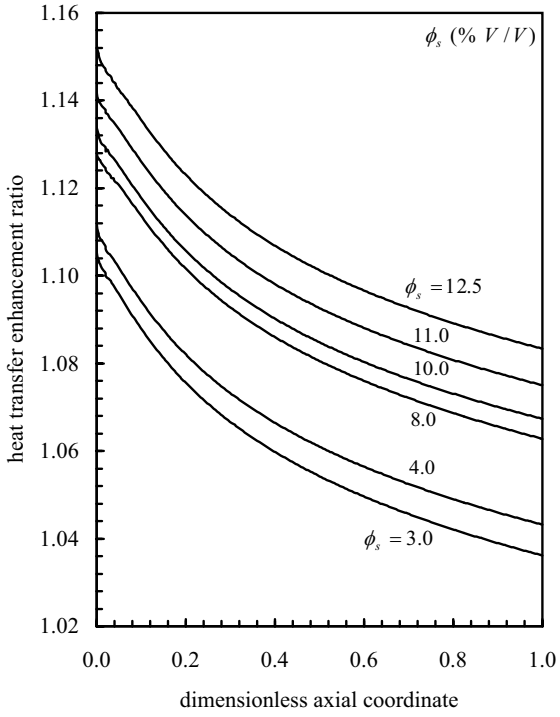

Figure 13. Heat transfer enhancement ratio (Nu_m/Nu_w) vs. dimensionless axial distance for different values of ASL ($\overline{\phi}_s$), at $Re = 20,000$, $L = 1.22$ m, $T_{in} = 50$ °C, $T_{w1} = 10$ °C.

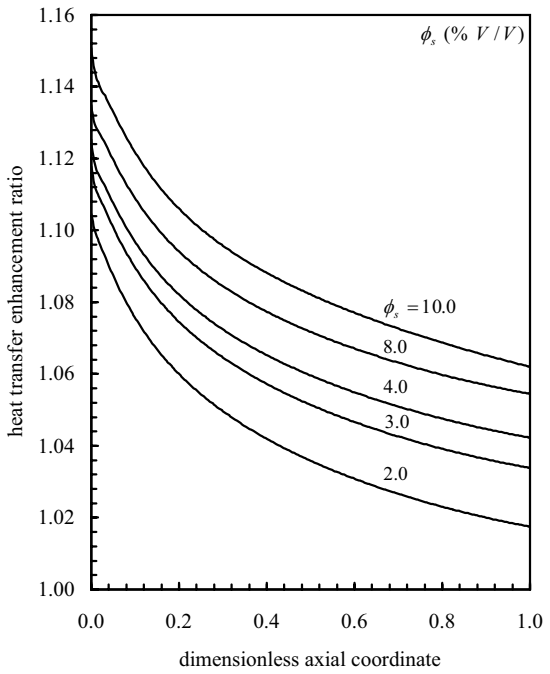

Figure 14. Heat transfer enhancement ratio ($\mathrm{Nu}_m/\mathrm{Nu}_w$) vs. dimensionless axial distance for different values of ASL ($\overline{\phi}_s$), at $Re = 20,000$, $L = 1.22$ m, $T_{in} = 70$ °C, $T_{w1} = 10$ °C.

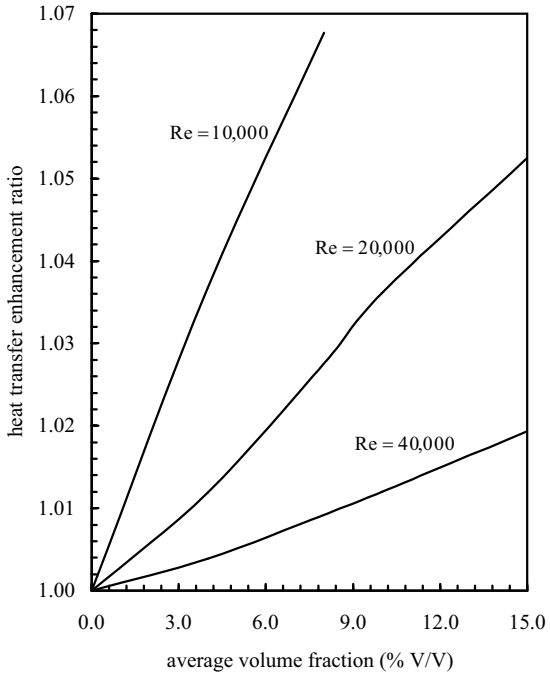

Figure 15. Heat transfer enhancement ratio ($\mathrm{Nu}_m/\mathrm{Nu}_w$) vs. ASL at different Reynolds numbers for $L = 1.22$ m, $T_{in} = 50$ °C, $T_{w1} = 10$ °C.

The Nusselt numbers for single phase (water) flows predicted from the present model are almost 8% greater than those obtained from a generalized correlation (Petukhov and Roizen, 1964). If the experimental single phase Nusselt numbers (Ozbelge and Köker, 1996) are compared with the same correlation, they are found to be 9% greater too. On the other hand, a qualitative comparison shows that experimental slurry heat transfer enhancement ratios (Ozbelge and Köker, 1996) are greater than the model predictions but the same trends are correctly predicted. It is thought that this discrepancy comes from using a continuum model that disregards the particle interactions. In addition, the experimental values for small aspect ratios might be expected to be uncertain because of the difficulty of obtaining perfect alignment of the inner pipe within the outer pipe and the disturbance of the flow by the devices that maintain alignment. It is not possible to make a one-to-one comparison between the experimental and predicted results, because the aspect ratios and hydraulic diameters of the annuli in the experimental work are in the ranges of 0.3-0.5 and 0.036-0.024 m, respectively, and RSDD data in these annuli were not available as its importance is indicated in our previous work (Eraslan and Ozbelge, 2003). Nevertheless, the present model provides sufficient information for some practical applications, such as heating or cooling slurries, for which detailed modeling would consume an unduly long time.

Conclusions

In this work, an attempt is made to predict the turbulent up-flow and heat transfer characteristics of dilute slurries through a concentric annulus of aspect ratio of 0.2 and hydraulic diameter of 0.1 m using experimental radial solid density distributions (RSDD) (Ozbelge and Beyaz, 2001). The calculations are performed by assuming zero solid densities at the walls of the annulus**,** and negligible shear stress in the laminar boundary layer near the walls. The assumption of negligible shear stress in the laminar viscous boundary layer besides the turbulent stresses was applied successfully in past modeling studies of dilute liquid-solid flows in a horizontal pipe (Michaelides and Farmer, 1984). As they reported, the model compared favorably with the experimental data of several different studies for homogeneous flow type. The only discrepancy observed was at very low velocities where settling of particles caused heterogeneous

type of flow in horizontal pipes. Since the present system is a vertical annulus, the dilute slurry flows in turbulent regime will be homogeneous for fine and moderate size particles (up to 250 μ), and, therefore, using a similar approach in the present modeling study can be justifiable. As a result, various important hydrodynamic and heat transfer characteristics of turbulent slurry up-flows were successfully predicted in this study. The present findings are that the radial location of maximum velocity is closer to the inner wall for slurries in comparison with the single phase flows and approaches further the inner wall with the increasing average solid loading (ASL) for a given Reynolds number. Frictional slurry pressure gradient and friction factor increase with ASL at constant Reynolds number. The heat transfer enhancement ratio increases with ASL at the same Reynolds number. In a turbulent flow regime, as the Reynolds number decreases the enhancement ratio increases for a given ASL. In other words, the effect of solids on the heat transfer enhancement becomes less important with increasing Reynolds number in turbulent flow.

Acknowledgment

The work by Ozbelge and Beyaz (1999) was financed by the Scientific and Technical Research Council of Turkey (TÜBİTAK; Project No: İNTAG-822) and partially by the Middle East Technical University; this support is greatly appreciated by the authors. Special thanks are extended to Prof. Dr. Turgut Tokdemir (in the Department of Engineering Sciences at M.E.T.U.) for his valuable comments. The help from Miss S. Erşahin with drawing the figures in the manuscript is acknowledged.

Nomenclature

ASL	average solids loading (plural: $ASLs$)
c	heat capacity, J/kg K
C_f	feed concentration of slurry, % (V/V)
$CDSPF$	constant density single phase fluid
D_H	hydraulic diameter, m
dP/dz	total pressure gradient, kg/m^{2}s^2
$(dP/dz)_{fm}$	frictional pressure gradient, kg/m^{2}s^2
f	friction factor, dimensionless
g	gravitational acceleration, m/s^2
h	heat transfer coefficient, W/m^2 K
L	length of test section, m
k	thermal conductivity, W/m K
N	number of grid points
Nu	Nusselt number, dimensionless
P	pressure, kg/m s^2
r	radial coordinate, m
r_M	radial location of maximum velocity and zero shear stress, m
r^*	dimensionless radial coordinate, $(r - r_1)/(r_2 - r_1)$
$RSDD$	radial solid density distribution (plural: $RSDDs$)
Re	Reynolds number
T	temperature, °C
T_{in}	inlet temperature of slurry, °C
u	velocity, m/s
u_{ave}	average velocity, m/s
X_s	local mass fraction of solids in the liquid phase, dimensionless
$VDSPF$	variable density single phase fluid
z	axial coordinate, m

Greek Letters

ϕ_s	local volume fraction of solids in the mixture, V/V
$\overline{\phi}_s$	volumetric average solid loading, % (V/V) or V/V
κ	Von Karman constant (= 0.4)
μ	viscosity, kg/m s
ρ	density, kg/m^3
τ	shear stress, kg/m s^2

Subscripts

b	bulk
l	liquid
m	mixture
p	particle
$w1$	inner wall

Superscripts

L	laminar
T	turbulent

References

Alajbegovic, A., Assad, A., Bonetto, F. and Lahey, R.T., "Phase Distribution and Turbulence Structure for Solid/Liquid Up-flow in a Pipe". Int. J. Multiphase Flow 20, 453-479, 1994.

Bird, R.B., Stewart, W. and Lightfoot, E.N., Transport Phenomena, John Wiley and Sons Inc., New York, 2002.

Boothroyd, R.G., Flowing Gas-Solids Suspensions, Chapman and Hall Ltd., London, 1971.

Brandon, C.A. and Thomas, D.G., "Transport Characteristics of Suspensions". Proc. 4th Int. Heat Transfer Conf., Paper CT-2.1, 1970.

Brighton, J.A. and Jones, J.B., "Fully Developed Turbulent Flow in Annuli". J. Basic Eng. Trans. ASME Series D 86, 835-842, 1964.

Eraslan, A.N. and Ozbelge, T.A., "Assessment of Flow and Heat Transfer Characteristics for Proposed Solid Density Distributions in Dilute Laminar Slurry Upflows through a Concentric Annulus". Chem Eng. Sci. 58, 4055-4069, 2003.

Garbow, B.S., Hillstrom, K.E. and More, J.J., "Testing Unconstrained Optimization Software". ACM Trans. Math. Software 7, 17-41, 1981.

Hestroni, G. and Rozenblit, R., "Heat Transfer to a Liquid-Solid Mixture in a Flume". Int. J. Multiphase Flow 20, 671-689, 1994.

Hinze, J.O., Turbulence, McGraw-Hill, New York, 1959.

Julian, F.M. and Dukler, A.E., "An Eddy Viscosity Model for the Friction in Gas-solid Flow". AIChE J. 11, 853-858, 1965.

Kofanov, V.J., "Heat Transfer and Hydraulic Resistance in Flowing Liquid Suspension in Pipes". Int. Chem. Eng. 4, 426-430, 1964.

McCabe, W.L., Smith, J.C. and Harriot, P., Unit Operations of Chemical Engineering. 5th ed., McGraw-Hill Int., Singapore, 1993.

Mehta, N.C., Smith, J.M. and Comings, E.W., "Pressure Drop in Air-Solid Flow Systems". Ind. & Eng. Chemistry 49, 986-992, 1957.

Michaelides, E.E., "Heat Transfer in Particulate Flows". Int. J. Heat Mass Transfer 29, 265-273, 1986.

Michaelides, E.E. and Farmer, L.K., "A Model for Slurry Flows Based on the Equations of Turbulence". J. Pipelines 4, 185-191, 1984.

Ozbelge, T.A., "The Location of Peak Heat Transfer Enhancement in Suspension Flows". Int. J. Multiphase Flow 19, 535-538, 1993.

Ozbelge, T.A. "Heat Transfer Enhancement in Turbulent Upward Flows of Liquid-Solid Suspensions through Vertical Annuli". Int. J. Heat Mass Transfer 44, 3373-3379, 2001.

Ozbelge, T.A. and Beyaz, A., (in Turkish) "Seyreltik Sıvı-katı Karışımlarının Akış Özellikleri". TÜBİTAK Project İNTAG-822, Report No: 196 I 010, Ankara, 1999.

Ozbelge, T.A. and Beyaz, A., "Dilute Solid-Liquid Upward Flows through a Vertical Annulus in a Closed-Loop System". Int. J. Multiphase Flow 27, 737-752, 2001.

Ozbelge, T.A. and Köker, S.H., "Heat Transfer Enhancement in Water-Feldspar Upflows through Vertical Annuli". Int. J. Heat Mass Transfer 39, 135-147, 1996.

Ozbelge, T.A. and Somer, T.G., "Hydrodynamic and Heat Transfer Characteristics of Liquid-Solid Suspensions in Horizontal Turbulent Pipe Flow". Chem. Eng. J. 38, 111-122, 1988.

Park, C.J., Choj, K.O. and Doh, D.S., "An Experimental and Theoretical Study on the Augmentation of Heat Transfer by Suspended Solid Particles in the Flowing Fluid in a Vertical Tube". Hwahak Konghak 27, 682-688, 1989.

Petukhov, B.S. and Roizen, L.I., "Generalized Relationship for Heat Transfer in a Turbulent Flow of Gas in Tubes of Annular Section". High Temp. 2, 65-68, 1964.

Plass, L. and Molerus, O, "Simultane Warmeübergangs und Druck Verlustmessungen an Feststoff / Flüssigkeits-Suspensionen im Übergangsbereich vom Homogenen zum Heterogenen Suspensions-Transport". Chem. Ing. Tech. 46, 355-356, 1974.

Roco, M.C., "Multiphase Flow: Summary Paper". Powder Technology 88, 275-284, 1996.

Rose, H.E. and Duckworth, R.A., "Transport of Solid Particles in Liquids and Gases". The Engineer 227, 392-478, 1969.

Sadatomi, M., Sato, Y. and Saruwatari, S., "Two-phase Flow in Vertical Noncircular Channels". Int. J. Multiphase Flow 8, 641-655, 1982.

Schlichting, H., Boundary Layer Theory, 6th Ed., McGraw-Hill, New York, 1968.

Smith, J.W. and Paradi, J.C., "Heat Transfer to Settling Slurries in Vertical Transport". J. Pipelines 3, 43-52, 1982.

Zandi, I., Advances in Solid-Liquid Flow in Pipes and Its Application, Pergamon Press, New York, 1971.